Study on SMO-based sensorless control f or two-axis precision positioning of a planar potion stage

Songyi Dian[1,#], Shuang Tian[1], Wei Gao[2], Weng Tao[1] and Hang Dong[1]

1 School of Electrical Engineering and Information Technology, Sichuan University, Chengdu, CHINA
2 Nano-Metrology and Control Laboratory, Department of Nanomechanics, Tohoku University, Aramaki Aza Aoba 6-6-01, Sendai, 980-8579 JAPAN
Corresponding Author / E-mail: scudiansy@scu.edu.cn, TEL: +86-28-85468208, FAX: +86-28-85468208

KEYWORDS : Sliding Mode Observer, Sensorless Control, Precision Positioning, Planar Motion Stage

Two-axis planar motion stages driven by Sawyer motor, being capable of good open-loop positioning resolution, rapid acceleration and high speed, have been widely used in the field of precision manufacturing and measurement such as wafer probing, surface measurement, automated assembly and precision machining. In this study, a novel partial sensorless control (PSC) has been tailored to two-axis precision positioning issue for Sawyer motor-based planar motion stage. For the position estimation, a Sliding Mode Observer (SMO) -based technique has been implemented. We investigate the positioning performance on open-loop control, closed-loop control and PSC by experiments. The results of experiments have verified that PSC is an available way to maintain travel range and reduce the cost for precise position sensing while without so much sacrifice on positioning acc uracy comparing with the mentioned other methods for the two-axis planar motion stage.

Manuscript received: January XX, 2011 / Accepted: January XX, 2011

1. Introduction

Two-axis planar motion stages driven by Sawyer motor have been widely used in the field of precision manufacturing and measurement such as wafer probing, surface measurement, automated assembly and precision machining in recent years. This type stage is capable of two or above degree-of-freedom (DOF) motion in a plane, good open-loop positioning resolution, rapid acceleration and high speed. When operated in open-loop control, however, it is easy to miss steps, has long settling time, and has low-disturbance rejection and degraded performance due to unwanted yawing motion and possible loss of synchronization between the mover and platen teeth.[1,2] Consequently, closed-loop control and other advanced control methods for these stages have recently been addressed.[3-6] By these methods, not only many disadvantages encountered during open-loop control have been overcome, but also positioning performance has been improved up to sub-micron order. For the purpose of constructing closed-loop control, position sensing is necessary. Multi-axis interferometer systems or other mechanical/optical sensors such as encoders have been used in planar motion stages for precision measurement. These sensing methods, however, always increase cost and size of these stages.[7] Especially these sensors limit the travel range because this range for the moving element of stage is always decided by cross-action of optical beam or multi sensors. To overcome the above shortcomings of current precision position-sensing, many achievements have been done by using sensorless control.[8-10] However, up to now the sensorless control method was only used in open-loop mode and the test was conducted only in single-axis motion stage.

In this paper, we construct a novel partial sensorless control (PSC) for Sawyer motor-based two-axis planar motion stage. One-axis laser interferometer has been utilized to measure one translational motion and one yawing motion, and then to construct feedback control for the above motions. Meanwhile, another translational motion constructs closed-loop control based on essential estimated parameters instead of position-sensing for this motion. In order to achieve these parameters by sensorless method, a SMO-based component has been implemented. We investigate the positioning performance comparison by applying PSC, open-loop control in all-axis and position sensing-based closed-loop control in all-axis respectively to the motion stage experimentally. The results of experiments have verified the effectiveness of PSC scheme in the planar motion stage.

2. Two-Axis Planar Motion Stage

Fig. 1 shows a photograph of the planar motion stage driven by Sawyer motor. The Sawyer motor consists of a passive steel platen etched with a waffle-iron type pattern, and a mover with three symmetrically mounted forcers (showed as in Fig. 2, named X forcer,

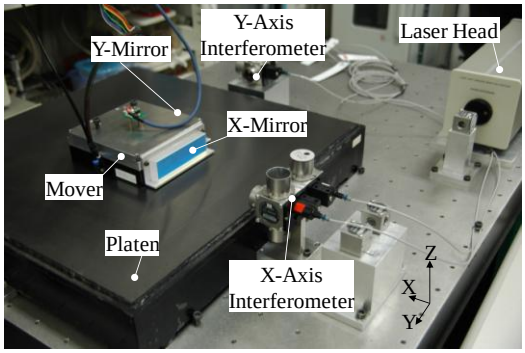

Fig. 1 Photo of Sawyer motor-driven two-axis motion stage

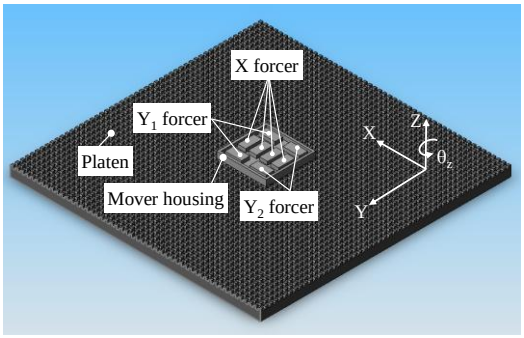

Fig. 2 Schematic view of the inner structure of the mover

Y1 forcer and Y2 forcer, respectively). The forcers generate driving forces against the motor platen: X forcer provides driving force for X-motion; Y1 and Y2 forcers not only provide driving force for Y-motion but also generate an unwanted moment for yawing motion while the two forcers are driven in opposite direction. Dynamic modeling of the stage has been done in the reference 11.

3. Position and Speed Estimation by SMO

3.1 D-Q Modeling of Sawyer Motor

It is essential to obtain a linear D-Q model for the purpose of sensorless control. In this study, X-motion is chosen to be the translational motion controlled by estimation position. The state space representation the model of X-motion is given by Eq. (1):

$$\begin{aligned}
\frac{di_a}{dt} &= -\frac{R}{L}i_a - \frac{K_f}{L}\cos(\frac{2\pi}{p}x)v + \frac{u_a}{L} \\
\frac{di_b}{dt} &= -\frac{R}{L}i_b - \frac{K_f}{L}\sin(\frac{2\pi}{p}x)v + \frac{u_b}{L} \\
\frac{dv}{dt} &= \frac{K_f}{m}i_a\cos(\frac{2\pi}{p}x) + \frac{K_f}{m}i_b\sin(\frac{2\pi}{p}x) \\
\frac{dx}{dt} &= v
\end{aligned} \tag{1}$$

In Eq. (1), i_a and i_b: currents of phases A and B of the coils of X forcer [A]; u_a and u_b: phase voltages of phases A and B [V]; R: phase resistance [Ω]; L: phase inductance [H]; K_f: thrust constant [N/A]; m: mover mass [kg]; x: actual position of the forcer [m]; v: actual speed of the forcer [m/s]; p: teeth pitch of the platen [m]. Applying the Park transformation as Eq. (2) on Eq. (1) gives directly the D-Q model as Eq. (3):

$$\begin{bmatrix} w_d \\ w_q \end{bmatrix} = \begin{bmatrix} \cos(\frac{2\pi}{p}x) & \sin(\frac{2\pi}{p}x) \\ -\sin(\frac{2\pi}{p}x) & \cos(\frac{2\pi}{p}x) \end{bmatrix} \begin{bmatrix} w_a \\ w_b \end{bmatrix} \tag{2}$$

$$\begin{aligned}
\frac{di_d}{dt} &= -\frac{R}{L}i_d + \frac{2\pi}{p}i_q v - \frac{2K_f}{L}v + \frac{u_d}{L} \\
\frac{di_q}{dt} &= -\frac{R}{L}i_q - \frac{2\pi}{p}i_d v + \frac{u_q}{L} \\
\frac{dv}{dt} &= \frac{K_f}{m}i_d \\
\frac{dx}{dt} &= v
\end{aligned} \tag{3}$$

3.2 Feedback linearization of Sawyer motor

The nonlinearities on the model are now reduced only to some items in the two first equations of Eq. (3). These non-linearity items can be removed by feedback linearization using Eq. (4):

$$\begin{aligned}
u_d &= u_d^* - L\frac{2\pi}{p}i_q v + x \\
u_q &= u_q^* + L\frac{2\pi}{p}i_d v + x
\end{aligned} \tag{4}$$

Then Eq. (3) can be rewritten as Eq. (5):

$$\begin{aligned}
\frac{di_d}{dt} &= -\frac{R}{L}i_d - \frac{2K_f}{L}v + \frac{x}{L} + \frac{u_d^*}{L} \\
\frac{di_q}{dt} &= -\frac{R}{L}i_q + \frac{x}{L} + \frac{u_q^*}{L} \\
\frac{dv}{dt} &= \frac{K_f}{m}i_d \\
\frac{dx}{dt} &= v
\end{aligned} \tag{5}$$

Eq. (5) gives a completely linearized system model of X-motion of Sawyer motor by Park transformation and a change of variable illustrated as Fig. 3. Introducing the state variables $X(t) = [i_d, i_q, v, x]^T$, output variables $Y(t) = [i_d, i_q]^T$, input variables $U(t) = [u_d^*, u_q^*]^T$, the nominal state-space equation can be expressed by Eq. (6):

$$\begin{cases} \dot{X}(t) = AX(t) + BU(t) \\ Y(t) = CX(t) \end{cases} \tag{6}$$

where,

$$A = \begin{bmatrix} -\frac{R}{L} & 0 & -\frac{2K_f}{L} & \frac{1}{L} \\ 0 & -\frac{R}{L} & 0 & \frac{1}{L} \\ \frac{K_f}{m} & 0 & 0 & 0 \\ 0 & 0 & 1 & 0 \end{bmatrix} \qquad B = \begin{bmatrix} \frac{1}{L} & 0 \\ 0 & \frac{1}{L} \\ 0 & 0 \\ 0 & 0 \end{bmatrix}$$

$$C = \begin{bmatrix} 1 & 0 & 0 & 0 \\ 0 & 1 & 0 & 0 \end{bmatrix}$$

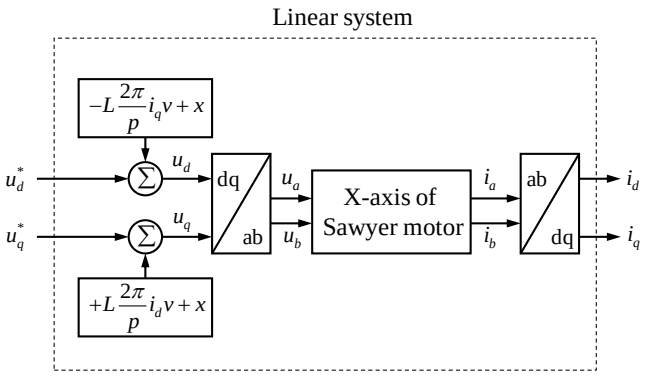

Fig. 3 Feedback linearization of Sawyer motor (X-axis)

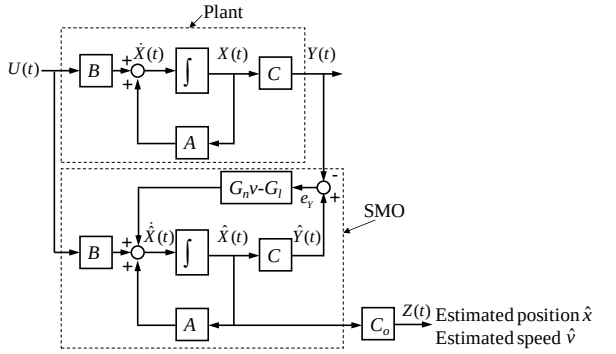

Fig. 4 Block diagram of the estimation principle for position and speed based on SMO

3.3 Position and Speed Estimation by SMO

According to the reference 12, there exists a linear change of coordinates T_o in which the system triple (A, B, C) of the nominal state-space equation as Eq. (6) has the structure list in Eq. (7):

$$T_o A T_o^{-1} = \begin{bmatrix} A_{11} & A_{12} \\ A_{21} & A_{22} \end{bmatrix} \quad T_o B = \begin{bmatrix} 0 \\ B_2 \end{bmatrix} \quad C T_o^{-1} = \begin{bmatrix} 0 & I_p \end{bmatrix} \tag{7}$$

Eq. (6) can thus be re-written as Eq. (8):

$$\begin{cases} \dot{X}_1(t) = A_{11} X_1(t) + A_{12} Y(t) + B_1 U(t) \\ \dot{Y}(t) = A_{21} X_1(t) + A_{22} Y(t) + B_2 U(t) + B_2 \xi \end{cases} \tag{8}$$

Where $X_1 \in \Re^{(n-p)}$, $Y \in \Re^p$ and the matrix A_{11} has stable eigenvalues.

A state observer proposed in the reference 12 is employed for Eq. (6) as Eq. (9):

$$\dot{\hat{X}}(t) = A\hat{X}(t) + BU(t) - G_l(C\hat{X}(t) - Y(t)) + G_n \upsilon \tag{9}$$

where the linear gain G_l and the nonlinear gain G_n can be written as Eq. (10):

$$G_l = T_o^{-1} \begin{bmatrix} A_{12} \\ A_{22} - A_{22}^s \end{bmatrix} \quad G_n = T_o^{-1} \begin{bmatrix} 0 \\ I_p \end{bmatrix} \tag{10}$$

A_{22}^s in Eq. (10) is a stable design matrix. If $P_2 \in \Re^{p \times p}$ is a symmetric positive definite Lyapunov matrix for A_{22}^s, the discontinuous output error injection υ can be defined by Eq. (11):

$$\upsilon = \begin{cases} -\rho(t, X(t), U(t)) \|B_2\| \dfrac{P_2 e_Y}{\|P_2 e_Y\|} & e_Y \neq 0 \\ 0 & e_Y = 0 \end{cases} \tag{11}$$

where $e_Y = \hat{Y} - Y$ is the output estimation error. The function ρ represents an upper bound on the magnitude of $\xi(t, X(t), U(t))$. For Eq. (9), the interesting output values of the constructed observer are position $\hat{x}$ and speed $\hat{v}$ of the mover, this leads to the observer output as Eq. (12):

$$\hat{Z}(t) = \begin{bmatrix} 0 & 0 & 1 & 0 \\ 0 & 0 & 0 & 1 \end{bmatrix} \hat{X}(t) = \begin{bmatrix} \hat{v} \\ \hat{x} \end{bmatrix} \tag{12}$$

The observer state-space equation is concluded as the form Eq. (13) based on Eq. (9) and Eq. (12):

$$\begin{cases} \dot{\hat{X}}(t) = A\hat{X}(t) + BU(t) + G_n \upsilon - G_l(C\hat{X}(t) - Y(t)) \\ \hat{Z}(t) = C_o \hat{X}(t) \end{cases}$$
$$C_o = \begin{bmatrix} 0 & 0 & 1 & 0 \\ 0 & 0 & 0 & 1 \end{bmatrix} \tag{13}$$

The estimation principle of position and speed based on SMO can be depicted by Fig. 4. If the state estimation error $e_1 = \hat{X}_1 - X_1$, the state estimation error and output error equation can be written as Eq. (14) and Eq. (15):

$$\dot{e}_1(t) = A_{11} e_1(t) \tag{14}$$

$$\dot{e}_Y(t) = A_{21} e_1(t) + A_{22}^s e_Y(t) + \upsilon - B_2 \xi \tag{15}$$

Because $e_Y = 0$ and $\dot{e}_Y = 0$ during the sliding motion, Eq. 15 becomes:

$$0 = A_{21} e_1(t) + \upsilon_{eq} - B_2 \xi \tag{16}$$

where υ_{eq} is the so-called equivalent output injection signal. The equivalent output injection represents the average behavior of the discontinuous component υ and represents the effort necessary to maintain the motion on the sliding surface. From Eq. 11 and using the fact that A_{11} is stable, it follows that $e_1(t) \to 0$. It means that the estimation position and estimation speed can be approached precisely to the actual position and speed. Moreover, the precisely estimation position and speed can be used in the closed-loop control of X-motion of the Sawyer motor-based stage.

3.5 Quadratic stability of the SMO

Let $Q_1 \in \Re^{p \times p}$ and $Q_2 \in \Re^{p \times p}$ be symmetric positive definite design matrices and as defined above, P_2 is the unique symmetric positive definite solution of the Lyapunov equation.

$$P_2 A_{22}^s + (A_{22}^s)^T P_2 = -Q_2 \tag{17}$$

$\hat{Q}$ can be defined by using the computed value of P_2 as

$$\hat{Q} = A_{21}^T P_2 Q_2^{-1} P_2 A_{21} + Q_1 \tag{18}$$

where $\hat{Q} = \hat{Q}^T > 0$. Let $P_1 \in \Re^{(n-p)\times(n-p)}$ be the unique symmetric positive definite solution to the Lyapunov equation

$$P_1 A_{11} + (A_{11})^T P_1 = -\hat{Q} \tag{19}$$

In order to verify the stability of the observer on the sliding mode surface, consider the following candidate Lyapunov function:

$$V(e_1, e_Y) = e_1^T P_1 e_1 + e_Y^T P_2 e_Y \tag{20}$$

The derivative along the system trajectory

$$\dot{V} = -e_1^T \hat{Q} e_1 + e_1^T A_{21}^T P_2 e_Y + e_Y^T P_2 A_{21} e_1 - e_Y^T Q_2 e_Y + 2e_Y^T P_2 \upsilon - 2e_Y^T P_2 B_2 \xi \tag{21}$$

It can be found that

$$\begin{aligned} &(e_Y - Q_2^{-1} P_2 A_{21} e_1)^T Q_2 (e_Y - Q_2^{-1} P_2 A_{21} e_1) \\ &\equiv e_Y^T Q_2 e_Y - e_1^T A_{21}^T P_2 e_Y - e_Y^T P_2 A_{21} e_1 + e_1^T A_{21}^T P_2 Q_2^{-1} P_2 A_{21} e_1 \end{aligned} \tag{22}$$

Substituting the identity (22) into Eq. (21) and writing for notational convenience $(e_Y - Q_2^{-1} P_2 A_{21} e_1)$ as $\tilde{e}_Y$ then

$$\begin{aligned} \dot{V} &= -e_1^T \hat{Q} e_1 + e_1^T A_{21}^T P_2 Q_2^{-1} P_2 A_{21} e_1 - \tilde{e}_Y^T Q_2 \tilde{e}_Y + 2e_Y^T P_2 \upsilon - 2e_Y^T P_2 B_2 \xi \\ &= -e_1^T Q_1 e_1 - \tilde{e}_Y^T Q_2 \tilde{e}_Y + 2e_Y^T P_2 \upsilon - 2e_Y^T P_2 B_2 \xi \\ &= -e_1^T Q_1 e_1 - \tilde{e}_Y^T Q_2 \tilde{e}_Y - 2\rho(t, X, U) \|B_2\| \|P_2 e_Y\| - 2e_Y^T P_2 B_2 \xi \\ &< 0 \qquad for\ (e_1, e_Y) \neq 0 \end{aligned} \tag{23}$$

And hence the error system of the SMO is quadratically stable.

3.6 Partial Sensorless Control Scheme of the Two-Axis Planar Motion Stage

For constructing closed-loop control, Y-axis and θ_z-axis use the interferometer to measure the position of Y- and θ_z- directions, while the position of X-axis is acquired by SMO-based estimation algorithm instead of using interferometer. The structure of PSC shows in Fig. 5.

The broken-line block of Fig. 5 shows a full implementation of speed and position control loops using the estimated values of speed and position for X-motion. A SMO which implemented by Eq. (15) is used to estimate the position and speed of X-motion using the measurement values of motor phase currents (i_a, i_b) and control input commands (u_d^*, u_q^*). In this scheme, i_q^* is set to constant zero. After the commutation of position control and speed control, (u_d^*, u_q^*) can be decided. In order to obtain the D-Q input commands (u_d, u_q), the estimated position and speed are used as the position x and the speed in Eq. (4). The actual input commands (u_a, u_b) can transfer from (u_d, u_q) by Park inverse transform and then provide to micro-stepping drive. Similarly, in order to obtain D-Q currents (i_d, i_q), actual phase currents (i_a, i_b) are measured and then transferred to D-Q currents (i_d, i_q) by Park transform. Meanwhile, general PID control based on positions measured by interferometer is adopted for Y-motion and θ_z -motion, respectively.

4. Experiment Results

4.1 Experiment Setup

The block diagram of the experimental system is outlined in Fig. 6. The control algorithm is implemented on a DSP (TMS320C6701) board running at 167 MHz, and the resulting control effort is converted to an analog signal by a 16-bit D/A board. The measuring task for the motion of the mover is carried out by a multi-axis laser interferometer measurement system with 0.625 nm resolution. For PSC, X-interferometer is used only for comparison between estimated position and actual position. For open-loop control, both X- and Y-interferometers are used only for comparison.

4.2 Positioning Performance Comparison

Fig. 7 shows the comparison of positioning capability while the stage is controlled by PSC, open-loop control in all-axis respectively. Fig. 7 (a) shows the comparison between estimated position by SMO and measured position when using PSC. From the figure, good match between the actual position and the SMO-based estimated position by PSC has been confirmed. Fig. 7 (b) is the result of 3 μm ramp-motion by different control methods.

In Fig. 7 (b), position error of about 0.25 μm is obtained when PSC is used; while it has been measured up to about 2.5 μm under open-loop control (OLC). The experimental results confirm that the positioning performance under PSC is much better than the one under OLC. The positioning performance comparison by open-loop control in all-axis, PSC and position sensing-based closed-loop control in all-axis (The positioning capability while controlled by closed-loop control in all-axis can be referred in the reference 11) is list at Table 1.

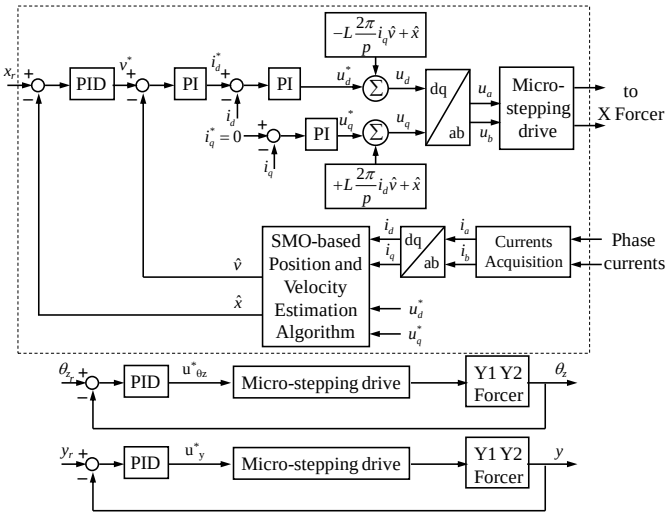

Fig. 5 Overall structure of partial sensorless control (PSC)

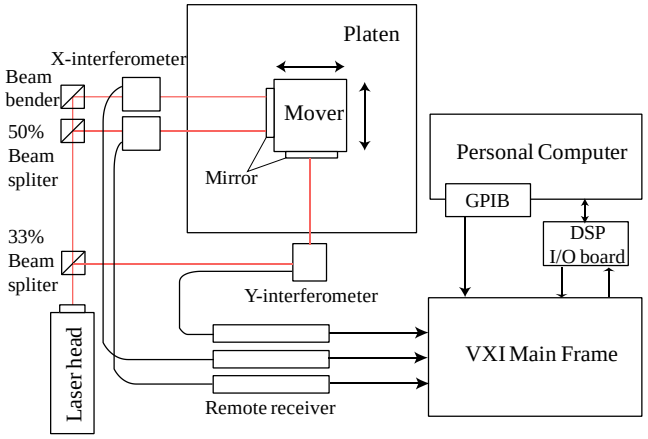

Fig. 6 Schematic diagram of the experimental setup

4.2 Consecutive-step responses by PSC

Fig. 8 shows the mover responses to 250 nm consecutive step commands applied at a time interval of 0.5 s. From the figure, it can be seen that the planar motion stage has the ability of sub-micron positioning by PSC.

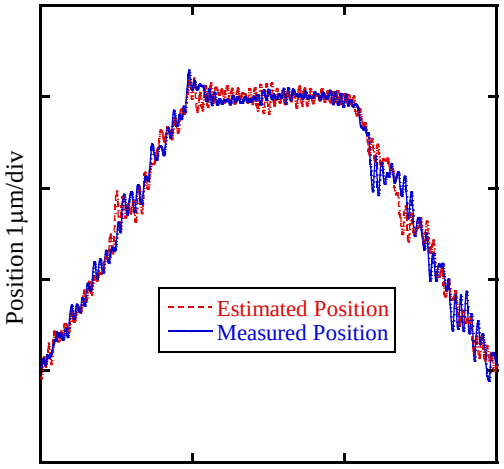

(a)

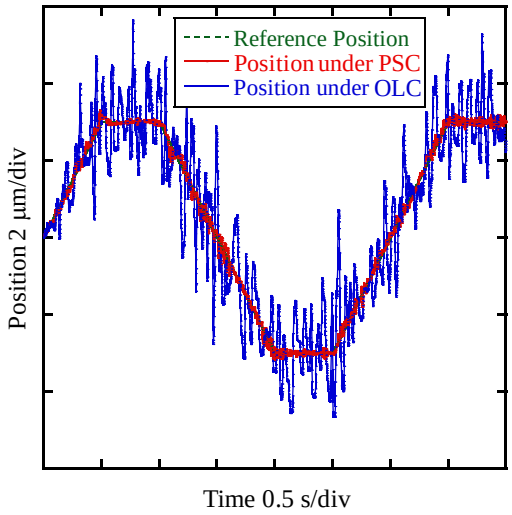

(b)

Fig. 7 Positioning performance at X-motion: (a) Comparison of th e estimated position by SMO and the measured position when usi ng PSC; (b) Position comparison by different control methods.

Table 1 Positioning performance comparison by different control methods.

Control methods	Positioning accur acy [μm]	Travel range in X-and Y-axes [mm]
Open-loop control in all-axis	2.5	300×300
PSC	0.25	300×300
Closed-loop control in all-axis	0.1	100×100

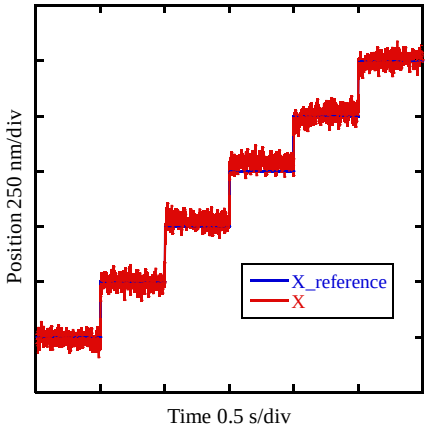

Fig. 8 250-nm consecutive step for X-direction by PSC

5. Conclusions

The paper focuses on a novel sensorless control of Sawyer motor-based two-axis planar motion stage for precision positioning. D-Q modeling and linearization of Sawyer motor have been performed to obtain a completely linear and observable model. The principle of position and speed estimation based on SMO has been investigated. The quadratic stability of the SMO has also been discussed. Then the partial sensorless closed-loop control method for two axes motions (one axis motion closed-loop controlled by measured position, another axis motion closed-loop controlled by estimated position) has been constructed and implemented by DSP for Sawyer motor-based planar stage. Experiment results have shown that the planar motion stage has the ability of sub-micron positioning accuracy (about 0.25 μm) by PSC compared with the positioning accuracy (about 2.5 μm) by open-loop control and the one (about 0.1 μm) by two-axis position sensing-based closed-loop control. The travel range of the mover in X- and Y- axes by PSC is same as the one by open-loop control and bigger than the one by two-axis position sensing-based closed-loop control. It is confirmed that PSC is an available way to maintain travel range and reduce the cost for position sensing while without so much sacrifice on positioning accuracy comparing with position sensing-based closed-loop control for two-axis planar motion stage.

REFERENCES

1. Pelta, E., “Two-axis Sawyer motor for motion systems,” IEEE Control Systems Magazine, Vol. 7, No. 5, pp.20-24, 1987.
2. Soltz, M. A., Yao, Y. L. and Ish-Shalom, J., “Investigation of a 2-D planar motor based machine tool motion system,” Int. J. of Machine Tools & Manufacture Vol. 39, No. 7, pp.1157-1169, 1999.
3. Gao, W., Tano, M., Kiyno, S., Tomita, Y. and Sasaki, T., “Precision positioning of a Sawyer motor-driven stage,” J. of Japan Society for Precision Engineering, Vol. 71, No. 4, pp.523-527, 2005.
4. Tano, M., Gao, W., Dian, S., Kiyono, S., Tomita, Y., Makino, K. and Motita, H., “Construction of a measurement and control system for a Sawyer motor-driven planar motion stage,” Nanotechnology and Precision Engineering, Vol. 4, No.3, pp.182-189, 2006.

5. Krishinamurthy, P. and Khorrami, F., "Robust adaptive control of Sawyer motors without current measurements," IEEE/ASME Transactions on Mechatronics, Vol. 9, No. 4, pp.689-696, 2004.
6. Dian, S., Arai, Y. and Gao, W., "Precision positioning control of a Sawyer motor-based two-axis planar motion stage," Proc. 3rd International Conference on Positioning Technology, pp.143, 2008.
7. Gao, W. and Dian, S., "Precision control of planar motion stages -Design and implementation of precision motion control strategies-," VDM Verlag Dr. Müller, pp.91-143, 2010.
8. Yang, S. M. and Kuo, E. L., "Damping a hybrid stepping mot or with estimated position and velocity," IEEE Transactions on Power Electronics, Vol. 18, No. 3, pp.880-887, 2003.
9. Bendjedia, M., Ait-Amirat, Y., Walther, B. and A. Berthon, "Sensorless control of hybrid stepper motor," 2007 European Conference on Power Electronics and Applications, pp.1-10, 2007.
10. Hirai, J., Kim, T. W. and Kawamura, A., "Position-sensorless drive of linear pulse motor for suppressing transient vibration," IEEE Transactions on Industrial Electronics, Vol. 47, No. 2, p p.337-345, 2000.
11. Dian, S., Arai, Y. and Gao, W., "Precision positioning control of a Sawyer motor-based two-axis planar motion stage," Int. J. Surface Science and Engineering, Vol. 3, No. 3, pp.253-271, 200 9.
12. Edwards, C. and Spurgeon, S. K., "Sliding mode control - Theory and Applications-," Taylor & Francis, pp.147-153, 1998.